

COOPERATIVE UAS LOCALIZATION USING LOW COST SENSORS

Salil Goel^{a,b,*}, Allison Kealy^b, and Bharat Lohani^a

^a Department of Civil Engineering, Indian Institute of Technology Kanpur, Kanpur, Uttar Pradesh, India - (salilg, blohani)@iitk.ac.in

^b Department of Infrastructure Engineering, University Of Melbourne, VIC, Australia - a.kealy@unimelb.edu.au

Commission I, ICWG I/Vb

KEY WORDS: Cooperative Localization, Unmanned Aerial System, Kalman Filter, Centralized architecture, Distributed architecture, Covariance Intersection.

ABSTRACT:

Networks of small, low cost Unmanned Aerial Systems (UASs) have the potential to improve responsiveness and situational awareness across an increasing number of applications including defense, surveillance, mapping, search and rescue, disaster management, mineral exploration, assisted guidance and navigation etc. These ad hoc UAS networks typically have the capability to communicate with each other and can share data between the individual UAS nodes. Thus these networks can operate as robust and efficient information acquisition platforms. For any of the applications involving UASs, a primary requirement is the localization i.e. determining the position and orientation of the UAS. The performance requirements of localization can vary with individual applications, for example: mapping applications need much higher localization accuracy as compared to the applications involving only surveillance. The sharing of appropriate data between UASs can prove to be advantageous when compared to a single UAS, in terms of improving the positioning accuracy and reliability particularly in partially or completely GNSS denied environments. This research aims to integrate low cost positioning sensors and cooperative localization technique for a network of UASs. Our hypothesis is that it is possible to achieve high accurate, real-time localization of each of the nodes in the network even with cheaper sensors if the nodes of the network share information among themselves. This hypothesis is validated using simulations and the results are analyzed both for centralized and distributed estimation architectures. At first, the results are studied for a two node network which is then expanded for a network containing more number of nodes. Having more nodes in the network allows us to study the properties of the network including the effect of size and shape of the network on accuracy of the nodes.

1. INTRODUCTION

Unmanned Aerial Systems (UAS) are now being increasingly used in a number of applications including surveillance, mapping, defense, search and rescue, mineral exploration, disaster management, assisted guidance and navigation etc. To effectively use UAS or swarms of UAS in any of the applications, determining the correct position and orientation of the UAS (or all the UAS in the network) is of utmost importance. At present it is achieved by installing GNSS receivers along with some inertial sensors and processing the data collected by sensors using an appropriate filter such as Kalman Filter. Although UAS is an interesting technology which is yet to realize its full potential, a number of challenges need to be addressed before the technology can be efficiently used in any application. The existing challenges can be classified in to two categories namely, performance challenges and practical challenges. Performance challenges include: (i) Meter to Sub-meter positioning accuracy of current systems which is limiting its use in high accuracy demanding applications such as mapping, (ii) Poor reliability on the system, meaning the whole mission is at the risk of failure due to the failure of a single UAS, (iii) Degradation of the positioning accuracy in GNSS challenged environments. Practical challenges include: (i) Payload-power conundrum, i.e. more power is required to carry more payload and one needs a bigger battery to have more power which in turn increases the payload. This is limiting in the sense that not many sensors can be installed on a single UAS, (ii) Failure of one UAS results in mission failure which is not true in a network of UAS. Further as the size of the UAS becomes smaller, its payload capacity decreases and high accuracy sensors cannot be installed due to their heavy weights resulting in poor positioning accuracy

and thus resulting in the poor accuracy of the derived products. Also, smaller UAS are much more prone to system failure resulting in failure of the complete mission which can have devastating consequences especially in missions involving defense and search and rescue.

A network of UASs may be able to overcome the above mentioned challenges and they also offer much more advantages especially in terms of increased reliability, robustness and efficiency, meaning the mission for which UAS is being used wouldn't be compromised even if one of the UAS in a network of UASs fails or crashes. Further, a network of UASs is expected to improve the positioning accuracy (Roumeliotis and Bekey 2002) as well as aid those UASs which have lost access to the GNSS signal or are operating under GNSS challenged environments. Also a network of UASs can perform tasks such as search and rescue (Waharte et al. 2009, Chung and Burdick 2008), exploration and mapping (Rekleitis et al. 2003, Santamario et al.), surveillance (Sutton et al. 2008, Grocholsky et al. 2006, Jones 2009), disaster management and situational awareness (Maza et al. 2011, Kuntze et al. 2012), exploration of unknown environments (Rekleitis et al. 1997, Zheng et al. 2005) etc. much more efficiently and much faster as compared to a single UAS. A single UAS may not even be able to complete the tasks mentioned before because of the limited power available on-board. For all the above mentioned applications, the key component is accurate localization of all the nodes in the UAS network. In this paper we aim at improving the positioning accuracy of a network of UASs by sharing information cooperatively. This research focuses on developing a network of UASs by integrating low cost positioning sensors along with cooperative localization techniques with the hypothesis that it is possible to maintain a given accuracy for a longer period of time in the GNSS challenged environments for

*Corresponding author

each of the nodes in a network in real time only if all the nodes in the network share their information with all the other nodes. This paper analyzes the localization accuracy of the nodes in a cooperative network which is a function of the estimation architecture and algorithm employed, quality of available measurements and geometry of the network.

The researchers in Roumeliotis and Bekey (2002) and Bailey et al.(2011) proposed partially distributed EKF based estimation algorithms to compute the pose of the robots. Roumeliotis and Bekey (2002) uses relative position and heading of the robots as the measurements for cooperative localization while Bailey et al.(2011) uses laser scanner and bearing measurements for the updation stage. Some of the researchers like Rashidi and Mohammadloo (2011) have used range sensor measurements along with inertial sensors with in the centralized EKF estimation algorithm. Majority of these researchers (Roumeliotis and Bekey 2002, Bailey et al. 2011, Rashidi and Mohammadloo 2011) have solved the problem for two dimensional spaces and while neglecting or not using the observations of inertial measurement unit (IMU). A number of estimation algorithms including UKF (Shi et al. 2010), Covariance Intersection (Carrillo-Arce et al. 2013), Split Covariance Intersection (Wanasinghe et al. 2014, Li and Nashashibi 2013), Belief propagation (Savic and Zazo 2013), MAP (Nerukar et al. 2009), Iterated Kalman filter (Pillonetto and Carpin 2007) etc. have been used in the distributed estimation architecture. The work for distributed cooperative localization using ground based robots seems to be very extensive (Shi et al. 2010, Carrillo-Arce et al. 2013, Wanasinghe et al. 2014, Savic and Zazo 2013, Nerukar et al. 2009, Madhavan et al. 2002, Pilonetto and Carpin 2007, Bailey et al. 2011) but the work for airborne platforms seems to be somewhat limited (Indelman et al. 2012, Qu et al. 2010, Qu and Zhang 2011, Melnyk et al. 2012, Chen et al. 2013, Wan et al. 2015). Some of the researchers (Indelman et al. 2012, Melnyk et al. 2012) have attempted to use vision based sensors for cooperative localization.

In this research, we focus specifically on UAS which are installed with GNSS and inertial sensors. In addition, each of the UAS possesses a ranging and a communication sensor (like UWB or Wi-Fi). In what follows, we describe the mathematical framework for centralized fusion architecture for UAS and extend the same for distributed architecture. Unlike previous approaches, we present the results for a full 3D environment without neglecting the inertial sensor observations. Further we examine how the cooperative localization approaches affect the localization accuracy as compared to non-cooperative modes both in the GNSS available and challenged environments. Also, the centralized cooperative localization approaches are then compared with decentralized approaches and the pros and cons of each of the approaches are examined.

2. KINEMATIC MODEL

Before proceeding to describe the cooperative localization approaches, we will explain the mathematical structure of our state used in the proposed method and also provide details on the kinematic equations which form the basis of state space model. The state vector for i^{th} UAS in a network containing N UASs is a 16 dimensional state vector comprising of position, velocity, attitude, gyroscope drift, accelerometer bias and receiver clock bias. It is possible to choose a smaller state vector if one is only interested in positioning component and not the navigation component but we are interested in a general state including the navigation component. Thus the state vector for the i^{th} node can be written

as,

$$x^i = \begin{bmatrix} (r^i)^T & (v^i)^T & (\alpha^i)^T & (b_g^i)^T & (b_a^i)^T & (c_b^i)^T \end{bmatrix}^T \quad (1)$$

where the superscript ‘ T ’ denotes the transpose and superscript ‘ i ’ denotes the number of node (UAS) in the network. The notations r^i , v^i , α^i , b_g^i , b_a^i and c_b^i denote the position, velocity, attitude, gyroscope bias, accelerometer bias and receiver clock bias of the i^{th} UAS respectively. The equations of motion for a single node (UAS) can be written in ECEF frame as:

$$\dot{r}^e = v^e \quad (2)$$

$$\dot{v}^e = R_b^e f_b - 2\Omega_{ie}^e v^e + g^e \quad (3)$$

$$\dot{\alpha}^e = R_{\alpha^e} \omega_{ib} \quad (4)$$

where R_{α^e} is given by:

$$R_{\alpha^e} = \begin{bmatrix} 1 & \sin \phi \tan \theta & \cos \phi \tan \theta \\ 0 & \cos \phi & -\sin \phi \\ 0 & \sin \phi \sec \theta & \cos \phi \sec \theta \end{bmatrix}$$

where r^e denotes the position of the node in ECEF frame, v^e denotes the velocity and α^e denotes the attitude vector, Ω_{ie}^e denotes the skew symmetric matrix of the earth rotation vector in ECEF frame with respect to the inertial frame, R_b^e denotes the rotation vector from IMU body to ECEF frame and f_b denotes the observations taken by accelerometer on-board the node. Although it is easier to work in ECEF frame, working with NED frame may be more convenient in certain applications. Here, we choose ECEF as the reference frame but the same framework would be extended for NED frame or local navigation frame. The propagation model for biases are assumed to follow the markov property and can be written as follows,

$$(b_g)_{k+1} = (b_g)_k + w_g^k \quad (5)$$

$$(b_a)_{k+1} = (b_a)_k + w_a^k \quad (6)$$

$$(c_b)_{k+1} = (c_b)_k + w_{c_b}^k \quad (7)$$

where w^k denotes a random noise and follows any given distribution (e.g. normal distribution). Thus equations 2 to 4 and 5 to 7 can be combined to write,

$$\dot{x} = f(x, u, w) \quad (8)$$

where $f(x, y)$ denotes a nonlinear function of x and y and \dot{x} denotes the first derivative of x with respect to time. The notation u denotes the observations from IMU (i.e. accelerometer and gyroscope measurements).

3. CENTRALIZED COOPERATIVE LOCALIZATION

Extended Kalman Filter forms the basis of centralized cooperative localization. We use EKF only to demonstrate the centralized cooperative localization methodology and any other filter like UKF or Particle filter can be used instead of EKF within the same mathematical framework. Although we develop the mathematical framework for a general case having ‘ N ’ UASs in the network, we first demonstrate the framework for two UASs each of which is installed with GNSS, IMU, and Range and communication sensor. The same framework will then be extended for a network containing more number UASs in the network and the results will be then analyzed and compared with the cases when the UAS was not communicating with other nodes in the network.

3.1 State Space Model

In a centralized cooperative localization framework, the states and covariances of all the nodes (UAS) in the network is processed simultaneously at a centralized fusion center. Thus the joint state vector of all the ' N ' nodes can be written as,

$$X = \begin{bmatrix} (x^1)^T & (x^2)^T & \dots & (x^i)^T & \dots & (x^N)^T \end{bmatrix}^T$$

where x_i is given by equation 1. Thus equation 8 can be written for the joint state as,

$$\dot{X} = f(X, U, W) \quad (9)$$

Since we are using EKF for the centralized architecture, equation 9 can be linearized about a nominal state X_o using Taylor series expansion and thus state space model can be re-written in discretized form as follows,

$$X_{k+1} \approx F_k X_k + (f(X_o) - F X_o) \delta t + G_k W_k \delta t + B_k U_k \delta t \quad (10)$$

where $f(X_k)$ is the non linear function defining the state evolution, δt is the IMU sampling interval, $F_k = I + F \delta t$, F is the jacobian and is given as $F = \left. \frac{\partial f(X, W)}{\partial X} \right|_{X=X_o}$ and $W_k \sim N(0, S_k)$ is the noise vector. The noise vector W_k can be written as,

$$W_k = \begin{bmatrix} (w_k^1)^T & (w_k^2)^T & \dots & (w_k^i)^T & \dots & (w_k^N)^T \end{bmatrix}^T$$

where w_k^i can be written as follows,

$$w_k^i = \begin{bmatrix} w_{f_b} \\ w_{\omega_{ib}} \\ w_{b_a} \\ w_{b_g} \\ w_{c_b} \end{bmatrix}$$

where w_{f_b} and $w_{\omega_{ib}}$ denote the random errors in accelerometer and gyroscope sensors. The matrices F_k and G_k for a single node are given as,

$$F_k^i = \begin{bmatrix} I_{3 \times 3} & I_{3 \times 3} \delta t & 0_{3 \times 3} & 0_{3 \times 3} & 0_{3 \times 3} & 0_{3 \times 1} \\ 0_{3 \times 3} & (I_{3 \times 3} - 2\Omega_{ie}^e \delta t) & E \delta t & -R_b^e \delta t & 0_{3 \times 3} & 0_{3 \times 1} \\ 0_{3 \times 3} & 0_{3 \times 3} & I_{3 \times 3} + D \delta t & 0_{3 \times 3} & -R_{\alpha^e} \delta t & 0_{3 \times 1} \\ 0_{3 \times 3} & 0_{3 \times 3} & 0_{3 \times 3} & I_{3 \times 3} & 0_{3 \times 3} & 0_{3 \times 1} \\ 0_{3 \times 3} & 0_{3 \times 3} & 0_{3 \times 3} & 0_{3 \times 3} & I_{3 \times 3} & 0_{3 \times 1} \\ 0_{1 \times 3} & 0_{1 \times 3} & 0_{1 \times 3} & 0_{1 \times 3} & 0_{1 \times 3} & 1 \end{bmatrix} \quad (11)$$

$$G_k^i = \begin{bmatrix} 0_{3 \times 3} & 0_{3 \times 3} & 0_{3 \times 3} & 0_{3 \times 3} & 0_{3 \times 1} \\ R_b^e \delta t & 0_{3 \times 3} & 0_{3 \times 3} & 0_{3 \times 3} & 0_{3 \times 1} \\ 0_{3 \times 3} & R_{\alpha^e} \delta t & 0_{3 \times 3} & 0_{3 \times 3} & 0_{3 \times 1} \\ 0_{3 \times 3} & 0_{3 \times 3} & I_{3 \times 3} & 0_{3 \times 3} & 0_{3 \times 1} \\ 0_{3 \times 3} & 0_{3 \times 3} & 0_{3 \times 3} & I_{3 \times 3} & 0_{3 \times 1} \\ 0_{1 \times 3} & 0_{1 \times 3} & 0_{1 \times 3} & 0_{1 \times 3} & 1 \end{bmatrix} \quad (12)$$

where $E = -\frac{\partial(R_b^e b_a)}{\partial \alpha^e}$ and $D = -\frac{\partial(R_{\alpha^e} b_g)}{\partial \alpha^e}$. The matrix B_k and vector U_k in equation 10 are given as,

$$B_k^i = \begin{bmatrix} 0_{3 \times 3} & 0_{3 \times 3} \\ R_b^e & 0_{3 \times 3} \\ 0_{3 \times 3} & R_{\alpha^e} \\ 0_{3 \times 3} & 0_{3 \times 3} \\ 0_{3 \times 3} & 0_{3 \times 3} \\ 0_{1 \times 3} & 0_{1 \times 3} \end{bmatrix}$$

$$U_k^i = \begin{bmatrix} (f_b)_k \\ (\omega_{ib})_k \end{bmatrix}$$

With the assumption that none of the nodes affect the motion of any of the other nodes (UAS) i.e. each of the nodes is moving independently of its own and is not controlled by any of the other nodes, the state transition matrix (and other matrices) for the centralized fusion can be written as follows,

$$F_k = \begin{bmatrix} F_k^1 & 0 & \dots & \dots & 0 & 0 \\ 0 & F_k^2 & \dots & \dots & 0 & 0 \\ \dots & \dots & \dots & \dots & \dots & \dots \\ 0 & 0 & \dots & \dots & F_k^{N-1} & 0 \\ 0 & 0 & \dots & \dots & 0 & F_k^N \end{bmatrix}_{N \times N}$$

In the next subsection, we will demonstrate how the measurements are used to update the propagated states.

3.2 Measurement Model

The measurement model comprises of GNSS pseudorange measurements as well as relative range measurements among different nodes. Additionally, other relative measurements such as relative angles, relative position, overlapping images taken by different UASs can also be considered within the same mathematical framework. As of now, we restrict ourselves only to relative range measurements. Thus, the measurement model can be written as,

$$z_k^i = h(X_k^i) + e_k^i \quad (13)$$

where z_k^i denotes the measurement vector for the i^{th} UAS at the k^{th} time instant, $h(x)$ denotes the measurement function and e_k^i denotes a random measurement error following a certain distribution (which we assume to be normal). Thus, the measurement vector z_k^i can be written as below.

$$z_k^i = [\rho_1^i \quad \rho_2^i \quad \dots \quad \rho_{p_i}^i \quad d_{i1} \quad d_{i2} \quad \dots \quad d_{iq_i}]^T$$

where ρ_j^i denotes the pseudorange measurement from the j^{th} satellite to the i^{th} UAS and d_{ij} denotes the relative range measurement between node i and j . If at any given time, node i can see p_i satellites and can measure relative ranges to q_i different nodes, then the size of measurement vector is $(p_i + q_i)$. It is to be noted that the variable q_i described above as an upper limit of $(N - 1)$, since a single node can only take relative measurements from the remaining $(N - 1)$ nodes. Thus the joint measurement vector for all the nodes can be written as,

$$Z_k = \begin{bmatrix} (z_k^1)^T & (z_k^2)^T & \dots & (z_k^{N-1})^T & (z_k^N)^T \end{bmatrix}^T$$

For the general case of N UAS in a network where each node i can track p_i satellites and can communicate with q_i other nodes, the size of measurement vector will be $\sum_{i=1}^N (p_i + q_i)$ and the maximum possible size of measurement vector will be $\sum_{i=1}^N p_i + \binom{N}{2}$,

when each and every node in the network can measure its relative range with respect to every other node. The measurement function $h(x)$ can be broken down in to two different categories: One for satellite observations and second for relative range measurements. Thus, the measurement model can be written as follows,

$$\rho_p^i = \sqrt{(x_p - x^i)^2 + (y_p - y^i)^2 + (z_p - z^i)^2} + (c_b)^i + e_{\rho_p^i} \quad (14)$$

and

$$\hat{d}_{ij} = \sqrt{(x^i - x^j)^2 + (y^i - y^j)^2 + (z^i - z^j)^2} + e_{d_{ij}} \quad (15)$$

where \hat{d}_{ij} denotes the estimated distance between the two nodes i and j . Having defined the measurement model for each of the nodes, we can write the joint measurement model for centralized fusion as,

$$Z_k = h(X_k) + r_k \quad (16)$$

where Z_k denotes the joint measurements and X_k denotes the joint state vector. The linearized version of measurement model (equation 16) can be written as follows.

$$Z_k \approx H_k X_k + h(X_o) - H_k X_o + e_k \quad (17)$$

where X_o denotes the nominal state vector about which measurement model is linearized and H_k denotes the jacobian and is evaluated as $H_k = \left. \frac{\partial h(X_k)}{\partial X_k} \right|_{X_k=X_o}$. For example, for the case when there are only two nodes (i and j) in the network, the jacobian H_k can be written as follows.

$$H_k = \begin{bmatrix} H_k^{ii} & H_k^{ij} \\ H_k^{ji} & H_k^{jj} \\ H_k^{di} & H_k^{dj} \end{bmatrix} = \begin{bmatrix} \frac{\partial Z_k^i}{\partial X^i} & \frac{\partial Z_k^i}{\partial X^j} \\ \frac{\partial Z_k^j}{\partial X^i} & \frac{\partial Z_k^j}{\partial X^j} \\ \frac{\partial d_{ij}}{\partial X^i} & \frac{\partial d_{ij}}{\partial X^j} \end{bmatrix}$$

where H_k^{ij} denotes the jacobian at the k^{th} instant of the measurement vector of i^{th} node with respect to the state vector of the j^{th} node and H_k^{di} denotes the jacobian for the relative measurements with respect to the i^{th} node. Thus, the elements of the jacobian matrix are given as follows,

$$H_k^{ii} = \begin{bmatrix} \frac{\partial \rho_1^i}{\partial r^i} & 0_{1 \times 3} & 0_{1 \times 3} & 0_{1 \times 3} & 0_{1 \times 3} & 1 \\ \frac{\partial \rho_2^i}{\partial r^i} & 0_{1 \times 3} & 0_{1 \times 3} & 0_{1 \times 3} & 0_{1 \times 3} & 1 \\ \vdots & \vdots & \vdots & \vdots & \vdots & \vdots \\ \frac{\partial \rho_{p_i}^i}{\partial r^i} & 0_{1 \times 3} & 0_{1 \times 3} & 0_{1 \times 3} & 0_{1 \times 3} & 1 \end{bmatrix}_{p_i \times 16}$$

$$H_k^{ij} = \left[\frac{\partial Z_k^i}{\partial X^j} \right] = [0]_{(p_i) \times 16}$$

$$H_k^{di} = \left[\frac{\partial \hat{d}_{ij}}{\partial r^i} \quad 0_{1 \times 3} \quad 0_{1 \times 3} \quad 0_{1 \times 3} \quad 0_{1 \times 3} \quad 0 \right]$$

where p_i denotes the number of satellites tracked by the i^{th} node and $i \neq j$. Thus, the above example for 2 UAS in the network can be extended for any number of nodes in the network and the whole mathematical structure would remain intact. One could write a measurement super matrix H_k for N nodes in the network for a case when each and every node is visible to every other node in the network as follows.

$$H_k = \begin{bmatrix} H_k^{11} & 0 & 0 & \dots & \dots & \dots & 0 \\ 0 & H_k^{22} & 0 & \dots & \dots & \dots & 0 \\ \vdots & \vdots & \vdots & \dots & \dots & \dots & \vdots \\ 0 & 0 & 0 & \dots & \dots & \dots & H_k^{NN} \\ H_k^{d_{11}} & H_k^{d_{12}} & H_k^{d_{13}} & \dots & \dots & \dots & H_k^{d_{1N}} \\ \vdots & \vdots & \vdots & \dots & \dots & \dots & \vdots \\ H_k^{d_{(N)1}} & H_k^{d_{(N)2}} & H_k^{d_{(N)3}} & \dots & \dots & \dots & H_k^{d_{(N)N}} \end{bmatrix}$$

In the above super matrix, the notation $H_k^{d_{ji}} = \frac{\partial \hat{d}_{ij}}{\partial X^i}$ denotes the jacobian matrix for the i^{th} node and distance equation \hat{d}_{ij} between any two nodes m and n of the network. Obviously, some of the matrices $H_k^{d_{ji}}$ will be zero in the cases when the distance is measured between m and n and the jacobian is with respect to i , where $m \neq n \neq i$.

3.3 Centralized Extended Kalman Filter

We can use the standard Extended Kalman Filter (EKF) to cooperatively compute the states of all the UASs. The centralized

Kalman filter runs at a central processing center where all the measurements and observations from all the nodes (UASs) are received. After processing, the fusion center transmits back the states of each of the UASs. If some of the measurements (either the pseudorange or relative range) are not available, then those measurements are removed from the measurement vector. The standard prediction-correction model of EKF can be used to compute the states. It is to be noted that after the first update, the states of the UASs which have participated in the measurement update phase get correlated. This correlation will play an important role if one decides to distribute the above processing to all the nodes instead of processing them at the centralized processor, as has been demonstrated here. The importance of this correlation will be discussed in section 4..

4. DISTRIBUTED COOPERATIVE LOCALIZATION

Distributed approaches have attracted quite a significant attention from the researchers mostly because they are scalable and can account for increase (or decrease) in the network sizes. The computational complexity for centralized approaches increases exponentially with the increase in the number of nodes (UASs) which is limiting its applications. Also CL approaches have a single point of failure as compared to more robust distributed localization approaches.

A major challenge in distributed processing is the accurate estimation of correlations among the nodes in a network. Not taking in to account these correlations or an incorrect estimation of these correlations may result in the estimator getting inconsistent (Carrillo-Arce et al. 2013, Li and Nashashibi 2013) and may even cause the solution to diverge in some cases. Thus to implement distributed approaches, one has to either maintain a log of all the interactions occurring among all the nodes to keep track of the correlations or compute the correlation on demand, i.e. whenever two nodes come in contact with each other. In practice, keeping a log of interactions among the nodes requires a book keeping approach (Bahr and Walter 2009) and is not feasible in practice especially as the size of the network increases. Thus a number of methods focus on computing these correlation whenever two nodes come in contact with each other. These methods are called Covariance Intersection and Split Covariance Intersection methods (Carrillo-Arce et al. 2013, Wanasinghe et al. 2014, Li and Nashashibi 2013). A third category of algorithms exist which are inherently distributed in nature and come under the category of belief propagation methods (Savic and Zazo 2013, Chen et al. 2013, Wan et al. 2015). However in case of loopy networks, belief propagation methods may not result in exact inference (Savic et al. 2010) or may not even converge to the solution at all. While covariance (and split covariance) intersection methods do not suffer from this limitation and can perform equally well even in loopy networks. The state vector and kinematic equations for each of the UAS is the same as described in section 2.. In distributed CL, we are interested in estimating the state (and covariance) of each of the nodes individually instead of the joint state (and covariance) as was done in centralized CL method in section 3.. It is to be noted that instead of processing the data at a centralized fusion center as was done in centralized CL, the processing is distributed among all the nodes in the network i.e. each of the nodes runs a EKF and CI method locally and no centralized processor exists in this case. Having said that, in what follows we will describe the EKF-CI processing approach which is adopted at each of the nodes in the network.

4.1 Distributed Fusion: Covariance Intersection

Let at any time instant ‘ k ’ the state of any two UASs i and j in a network containing ‘ N ’ UASs is given by x_k^i and x_k^j , respectively and the corresponding covariances by P_k^i and P_k^j . Let these two nodes i and j communicate with each other and share relative information between them which can either be the relative distance, relative angle or relative position and orientation or any other information relating the states of nodes i and j . The objective is to then fuse this relative information with the states of either of the UASs and derive a new estimated state vector and corresponding covariance. One of the problems associated with distributed processing approaches (other than taking care of unknown correlation and loopy networks) is that it should be possible to express the state of node i explicitly using the relative information and the state of the other node j (Carrillo-Arce et al. 2013, Wanasinghe et al. 2014, Li and Nashashibi 2013). This disadvantage limits the use of distributed processing in the case when only implicit constraints are available between the two states, like the relative range measurement. In this paper we assume that the relative position is available to us by some means. Let us say we are interested in determining the state (and covariance) of the node i which has received relative information about itself from node j . Apart from sending the relative information, node j also shares its state and covariance information with node i . Now two estimates of the state of the node i at time ‘ $k + 1$ ’ are available: one from the time propagation of state space and second using the relative information. Here for simplicity we assume that the relative information contains only the relative position ‘ r_{rel}^{ij} ’, and is measured in global coordinate system. If the relative position is not in global coordinate system then it can be converted to the same using appropriate rotation matrices. Thus, the two estimates can be fused using the CI method where the fused estimate is given as,

$$(x_{k+1}^i)^+ = (x_{k+1}^i)^- + K_{k+1} \left[(x_{k+1}^i)^{rel} - H_{k+1} (x_{k+1}^i)^- \right] \quad (18)$$

where $(x_{k+1}^i)^-$ denotes the time propagated state of node i and is given by the time propagation model (Step-1) of EKF as described in section 3.3. The covariance corresponding to the state $(x_{k+1}^i)^-$ is given as $P_1^i = \frac{P_k^-}{W_1}$ where P_k^- is given in section 3.3, W_1 denotes a weighing factor and K_{k+1} is given by equation 21. The notation $(x_{k+1}^i)^{rel}$ denotes the estimate of node i obtained using the relative information and state of node j and is expressed mathematically as,

$$(x_{k+1}^i)^{rel} = H_{k+1} x_{k+1}^j + r_{rel}^{ij} \quad (19)$$

where H_{k+1} is similar to measurement matrix in a standard EKF and is given as,

$$H_{k+1} = \begin{bmatrix} 1 & 0 & 0 & 0 & \cdot & \cdot & \cdot & 0 \\ 0 & 1 & 0 & 0 & \cdot & \cdot & \cdot & 0 \\ 0 & 0 & 1 & 0 & \cdot & \cdot & \cdot & 0 \end{bmatrix} \quad (20)$$

The covariance corresponding to $(x_{k+1}^i)^{rel}$ is given as $P_2^i = \frac{P_{k+1}^{rel}}{W_2}$ where W_2 is a weighing factor and P_{k+1}^{rel} is given by the following expression,

$$P_{k+1}^{rel} = H_{k+1} P_{k+1}^j H_{k+1}^T + R_{k+1}^{rel}$$

where R_{k+1}^{rel} is the covariance matrix associated with the accuracy of relative information and in this case can be taken to be a diagonal (3×3) matrix and H_{k+1} is given by matrix in equation 20. The notation P_{k+1}^j denotes covariance matrix associated with the node j at the time instant $k + 1$. The notation K_{k+1}

in equation 18 is similar to kalman gain in a standard EKF and is given by the following expression,

$$K_{k+1} = P_1^i H_{k+1}^T \left(H_{k+1} P_1^i H_{k+1}^T + P_2^i \right) \quad (21)$$

The only unknown(s) in the equations 18 to 21 are W_1 and W_2 which are obtained through an optimization process which minimizes the trace (or determinant) of the covariance of the fused state estimate (Carrillo-Arce et al. 2013, Wanasinghe et al. 2014, Li and Nashashibi 2013). Thus optimization function can be mathematically expressed as,

$$\min \left[\text{tr} \left((I - K_{k+1} H_{k+1}) P_1^i \right) \right]_{\{W_1, W_2\}} \quad (22)$$

subject to the constraint that $\sum_{i=1}^N W_i = 1$. The notation $\text{tr}(x)$ denotes the trace of matrix x and all the other notations in equation 22 have already been defined. The optimization shown in equation 22 needs to be performed every time node i interacts with node j . It is to be noted that all the above mentioned processing takes place at node i and in the absence of any relative information or communication with any other node, the processing steps follow a standard EKF procedure.

5. RESULTS AND DISCUSSION

This section presents the results of the simulation both for centralized and distributed approaches and attempts to compare the two approaches as well as see the advantage(s) of information sharing (i.e. cooperative localization) over the cases when no information is shared.

5.1 Centralized Cooperative Localization

Let us first consider a case of two UASs in a network, both of which are equipped with GNSS and MEMS INS sensor as well as ranging and communication sensors. We assume that both the nodes are equipped with similar quality sensors. The UASs are flying at some distance apart from each other in a pre-defined pattern (as seen in figure 1). Figure 1 shows the XY plot of the trajectory followed by all the UASs in the network. During the flight, one of the nodes loses GNSS signal for some duration δt and relies on its inertial sensors. However, during this time period the UASs can communicate with each other and measure relative ranges to each other. After the time period δt , the UAS regains the GNSS signal while also communicating with the other UAS. We also present the results for the case when none of the nodes loses its GNSS signal and measures and communicates the relative distance between the two nodes and compares it to the case when no communication is done but both nodes have access to GNSS signal. The GNSS accuracy is assumed to be 2 cm in horizontal and 5 cm in vertical. The relative range is assumed to be accurate to 2 cm. The two nodes (UASs) send their state information (along

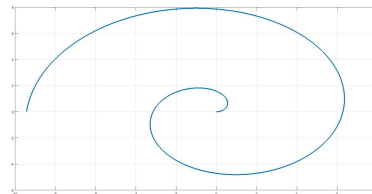


Figure 1: XY plot of the simulated trajectory of the UASs in the network.

with corresponding covariances), the data from respective GNSS and inertial sensors and relative range information to the central

fusion center which computes the joint state and covariance and passes it on to the corresponding nodes. Since the true trajectory of the UAS which lost its GNSS signal (referred to as the faulty UAS) is known to us, we can compute the advantage (to the faulty UAS) gained by information sharing and compare it to the case when no information was shared between the two nodes. Figure 2 shows a comparison of the error in the estimated position of one of the nodes when computed with information sharing (i.e. relative range or relative position is shared) and without information sharing while there was no loss of GNSS signal. As can be seen in figure 2 accuracy appears to be a little better in the case when range is shared between the two nodes, however this difference in accuracy is not much significant and it can be said that no significant improvement is obtained by sharing relative range when it is about as accurate as the GNSS information and there is no loss of GNSS signal. However, sharing relative position information does result in a significant improvement in the accuracy. The second case when one of nodes loses access to GNSS signal

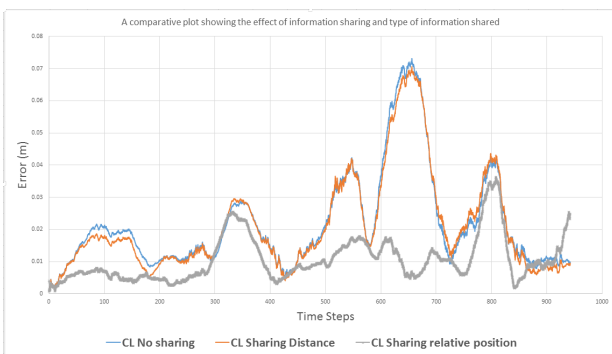


Figure 2: Error comparison for the position of a node for the case with and without information (relative range and relative position) sharing. The relative range accuracy in this case is assumed to be 2cm while relative position accuracy is about 5 cm and GNSS signal was available to both the nodes throughout the operation.

for a limited period but continues to communicate with the other node which has access to GNSS signal is presented in figure 3. As can be seen in figure 3, the UAS loses the GNSS signal at time step 100 and regains the signal at time step 500. The effect of information sharing is seen clearly here. The error in position continues to increase with time when GNSS signal is unavailable but the rate of increase of error is less in the case when (relative range) information is shared between the two UASs as compared to the case when there is no sharing of information. The relative range information in this case is not able to stop the error from increasing because relative range from one node only is not sufficient to solve for the position of the faulty node. However, if range information is available from 3 or more nodes or if relative position can be directly measured as will be demonstrated later, then the error in position of the faulty node can be contained. When the relative position information is shared instead of relative range, then it is observed that no deterioration in the accuracy is observed when GNSS signal is lost. This is of importance that it validates the hypothesis that cooperation among UASs may enable some nodes in the network to operate under GNSS denied regions.

5.1.1 Centralized fusion in a cooperative network: Let us include more nodes in a network and consider a network of n nodes where $n > 5$. The behavior of network changes with the connectivity, geometry and number of nodes in the network. Here we assume a fully connected network i.e. every node in a network is able to measure relative range to every other node. We con-

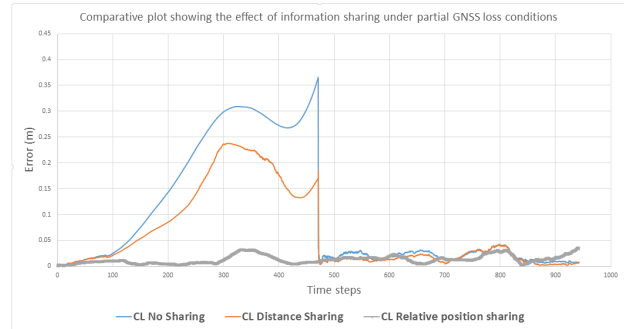


Figure 3: Error comparison for the position of a fault node which temporarily loses its GNSS signal for the case with and without information sharing. It also compares the cases for sharing relative range vs sharing relative position. The relative range accuracy in this case is assumed to be 2cm.

sider two scenarios: (1) When all the nodes in the network have GNSS availability, (2) When only few nodes have GNSS availability while all the other nodes can not access GNSS at all. Other simulation parameters remain the same as in the above cases. We present the results for the cases when there are 10 and 20 nodes in the network respectively, with variability in the nodes having access to GNSS signal. Figure 5 shows the error plots when GNSS

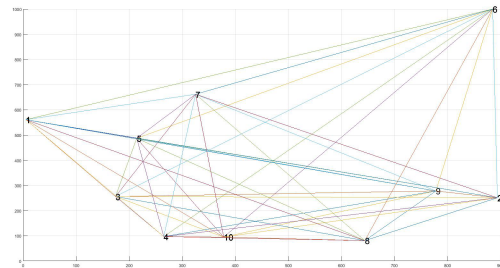


Figure 4: Network geometry at a given time instant with 10 nodes in the network with each node having full GNSS availability. The lines in the network represent the interactions between the nodes and the numbers represent the identification of the node.

is available to all the nodes while figure 6 shows the error plots when GNSS is available only to 50% of the nodes in the network. Thus nodes 1, 2, 4, 9, 10 have no GNSS access at all. It is interesting to note that even though these nodes have no GNSS through out the mission, the error remains bounded due to the information sharing. Also, the error for these nodes is not alike and is generally more than the nodes with GNSS. The reason for this is that the accuracy of a particular node is dependent on the relative position of the other nodes with respect to itself. The second interesting thing to note is that the maximum error in case of full GNSS availability is about 2 cm while in case of partial GNSS, it is about 25 cm. Similar pattern is observed when the number of nodes in the network are increased. As long as there are a minimum of 4 (or 3 in some cases) nodes with GNSS and the geometry of the network is sufficiently well, the error for all the nodes in the network will remain bounded. In the worst case scenario, if 4 nodes in a network have GNSS but all the 10 nodes lie in straight line, then this technique may not be able to stop the solution from diverging. Thus, the geometry of the network, relative accuracy of information shared and connectivity of the network plays an important role in determining the node localization accuracy.

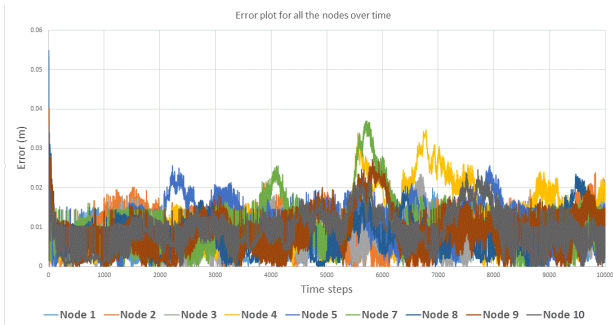


Figure 5: Error plots for all the nodes in the network assuming fully connected work and full GNSS availability.

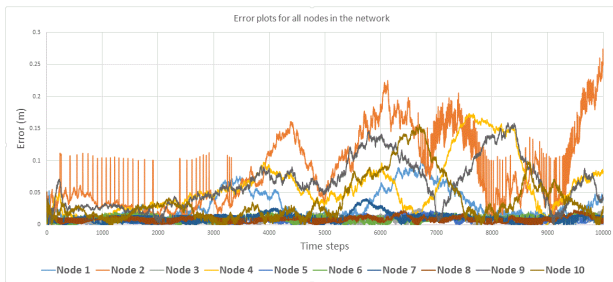


Figure 6: Error plots for all the nodes in the network assuming fully connected work and when GNSS is available only to 5 of the nodes.

5.2 Distributed Cooperative Localization

For distributed localization we only consider the case of relative position information sharing. Figure 7 shows the performance of distributed CI algorithm and also compares it with the case of centralized architecture. Further we consider two cases in distributed processing: (1) When GNSS is present on both the nodes, (2) When GNSS is present on only the first node. We are interested in studying the effect of having a GNSS on-board vs no GNSS while the relative position is shared. This is important in the sense that we can understand the effect of sharing information among the nodes in a distributed environment and how the accuracy is affected even if there are no GNSS outages. It is very clearly visible that having a GNSS on-board and also sharing relative information enhances the accuracy even in a distributed framework. In the following sections we will provide a comparison of centralized and distributed approaches.

5.3 Centralized vs Distributed framework

An interesting difference between the distributed and the centralized approaches (apart from the fact that processing is distributed) is that correlation is estimated in distributed approaches while this correlation is exactly available in the centralized approaches. Hence, it would be interesting to compare the performance of centralized and distributed approach based on EKF. To be fair, we choose the similar conditions for both, i.e. Only one of the nodes has access to GNSS and relative position information is shared. The only difference is that in one case, the processing is performed using centralized EKF approach while in the second case processing is performed in a distributed manner using EKF based on CI method. Figure 7 shows a comparison of the centralized processing with distributed processing. As expected, the centralized processing approach outperforms the distributed processing but at the expense of higher processing and communication cost. The reason for better accuracy in the centralized processing is due to the availability of joint covariance matrix and thus the exact correlation between the states is known which

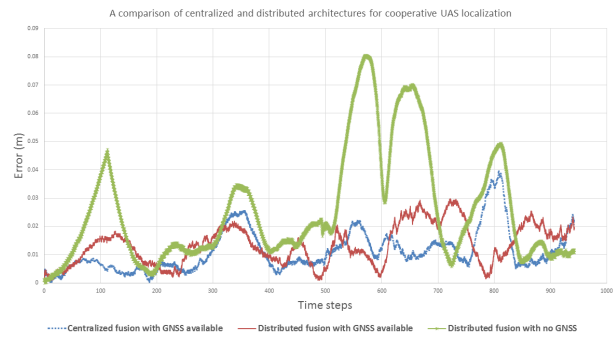


Figure 7: Error comparison for the position of a node when position information is shared by the node and there is no GNSS on-board for the case of centralized vs distributed processing.

is estimated by the CI algorithm in distributed processing. Although accuracy is better in CL approach, distributed approach offers other advantages like scalability, less communication and processing cost etc and applying CL approaches in a large network may pose computational challenges and may not be feasible. The centralized framework may be useful in cases when the network is relatively small and accuracy requirements are rather stringent. In the case when GNSS is available throughout, both the frameworks perform almost equally well. This is interesting because CL approaches achieve the similar accuracy as distributed approaches in GNSS available environments but at the expense of higher communication and processing costs. Thus, if GNSS is available and the nodes are capable of information sharing then it is advisable to implement a distributed localization architecture as compared to a centralized one.

6. CONCLUSIONS AND FUTURE WORK

This paper presented the first phase of research into which included a mathematical framework for centralized and distributed processing approaches for cooperative localization of a network of UAS which are equipped with low cost GNSS and MEMS based inertial sensors. The developed mathematical framework is analyzed using simulations and their performance studied. It is found that even when all the nodes of a network have access to GNSS signal, information sharing among the nodes may help in maintaining the consistent accuracy for a longer period of time under GNSS restricted environments depending on the quality and type of the information shared. Further, information sharing also assists UASs operating in GNSS challenged environments by allowing them to localize themselves. In general, centralized localization approach outperforms distributed approach because of the exact calculation of the correlations between the states of the UASs which are communicating with each other but at the expense of more communication and processing requirements. But distributed approaches can match the performance of CL approaches in GNSS available scenarios. Further, CL approaches are susceptible to failure because if the fusion center fails then all the nodes in the network will also fail resulting in a total collapse, while the same is not true for distributed approaches. In distributed approach, the processing is distributed among the nodes and each node is capable of operating independently. Thus if one node in a distributed approach collapses, other nodes in the network can continue operating without any impact on them. This makes the distributed approaches quite attractive. The future work would involve validation of the simulated results with field experiments.

REFERENCES

- Bahr, A., Walter, M. R., and Leonard, J. J., 2009. Consistent cooperative localization, in *IEEE International Conference on Robotics and Automation*, pp. 3415-3422.
- Bailey, T., Bryson, M., Mu, H., Vial, J., McCalman, L., and Durrant-Whyte, H., 2011. Decentralized cooperative localisation for heterogeneous teams of mobile robots, in *Proc. of the IEEE International Conference on Robotics and Automation*, Shanghai, China, pp. 2859-2865.
- Carrillo-Arce, L. C., Nerurkar, E. D., Gordillo, J. L., and Roumeliotis, S. I., 2013. Decentralized multi-robot cooperative localization using covariance intersection, in *IEEE/RSJ International Conference on Intelligent Robots and Systems*, pp. 1412 - 1417.
- Chen, X., Gao, W., and Wang, J., 2013. Robust all-source positioning of UAVs based on belief propagation, *EURASIP J. Adv. Signal Process.*, vol. 2013, no. 1, p. 150.
- Chung, T. and Burdick, J., 2008. Multi-agent probabilistic search in a sequential decision-theoretic framework, in *IEEE International Conference on Robotics and Automation (ICRA 2008)*, pp. 146 - 151.
- Grocholsky, B., Keller, J., Kumar, V., and Pappas, G., 2006. Cooperative air and ground surveillance, *IEEE Robotics and Automation Magazine*, vol. 13, pp. 16-25.
- Indelman, V., Gurfil, P., Rivlin, E., and Rotstein, H., 2012. Distributed vision-aided cooperative localization and navigation based on three-view geometry, *Rob. Auton. Syst.*, vol. 60, pp. 822-840.
- Jones, P. J., 2009. Cooperative area surveillance strategies using multiple unmanned systems, PhD thesis, Georgia Institute of Technology.
- Kuntze, H., Frey, C. W., Tchouhenkov, I., Staehle, B., Rome, E., Pfeiffer, K., Wenzel, A., and Wollenstein, J., 2012. Seneka-sensor network with mobile robots for disaster management, in *IEEE Conference on Technologies for Homeland Security (HST)*, pp. 406 - 410.
- Li, H. and Nashashibi, F., 2013. Cooperative multi-vehicle localization using split covariance intersection filter, *IEEE Intell. Transp. Syst. Mag.*, 5(2), pp. 3344.
- Madhavan, R., Fregene, K., and Parker, L. E., 2002. Distributed heterogeneous outdoor multi-robot localization, in *Proc. 2002 IEEE Int. Conf. Robot. Autom. (Cat. No.02CH37292)*, vol. 1, pp. 374-381.
- Maza, J. I., Caballero, F., Capitan, J., Ramiro Martinez de Dios, J., and Ollero, A., 2011. Experimental Results in Multi-UAV Coordination for Disaster Management and Civil Security Applications, *Journal of Intelligent and Robotic Systems*, 61(1-4), pp. 563 - 585.
- Melnyk, I. V., Hesch, J. A., and Roumeliotis, S. I., 2012. Cooperative vision-aided inertial navigation using overlapping views, in *Proceedings - IEEE International Conference on Robotics and Automation*, pp. 936 - 943.
- Nerurkar, E. D., Roumeliotis, S. I., and Martinelli, A., 2009. Distributed maximum a posteriori estimation for multi-robot cooperative localization, *IEEE Int. Conf. Robot. Autom.*, pp. 1402-1409.
- Pillonetto, G. and Carpin, S., 2007. Multirobot localization with unknown variance parameters using iterated Kalman filtering, *IEEE Int. Conf. Intell. Robot. Syst.*, pp. 1709-1714.
- Rashidi, A. J. and Mohammadloo, S., 2011. Simultaneous Cooperative Localization for AUVs Using Range-Only Sensors, *International Journal of Information Acquisition*, 8: 117 - 132.
- Rekleitis, I.M., Dudek, and Milios, G., E., 2003. Experiments in Free-Space Triangulation Using Cooperative Localization, *IEEE/RSJ/GI International Conference on Intelligent Robots and Systems (IROS)*.
- Rekleitis, I. M., Dudek, G., and Milios, E. E., 1997. Multi-robot exploration of an unknown environment, efficiently reducing the odometry error, in *Proc. 15th Int. Joint Conf. Artificial Intelligence (IJCAI-97)*, vol. 2, M. Pollack, Ed., Nagoya, Japan, pp. 1340 - 1345, Aug. 23-29.
- Roumeliotis, S. I. and Bekey, G. A., 2002. Distributed multi-robot localization, *IEEE Trans. Robot. Autom.*, 18(5), pp. 781-795.
- Santamario, E., Segor, F., and Tchouhenkov, I., 2013. Rapid Aerial Mapping with Multiple Heterogeneous Unmanned Vehicles, in *10th International ISCRAM Conference*, Germany.
- Savic, V. and Zazo, S., 2013. Cooperative localization in mobile networks using nonparametric variants of belief propagation, *Ad Hoc Networks*, 11(1), pp. 138 - 150.
- Savic V., Poblacin, A., Zazo, S., and Garca, M., 2010. Indoor Positioning Using Nonparametric Belief Propagation Based on Spanning Trees, *EURASIP J. Wirel. Commun. Netw.*, p. 963576.
- Shi, X., Wang, T., Huang, B., and Zhao, C., 2010. Cooperative multi-robot localization based on distributed UKF, in *Proc. - 2010 3rd IEEE Int. Conf. Comput. Sci. Inf. Technol. ICCSIT 2010*, vol. 6, pp. 590 - 593.
- Sutton, A., Fidan, B., and Van der Walle D., 2008. Hierarchical UAV formation control for cooperative surveillance, in *Proceedings of The 17th World Congress, The International Federation of Automatic Control*, Seoul, Korea, pp. 12087-12092.
- Qu, Y. and Zhang, Y., 2011. Cooperative localization against GPS signal loss in multiple UAVs flight, *J. Syst. Eng. Electron.*, 22(1), pp. 103-112.
- Qu, Y., Zhang, Y., and Zhou, Q., 2010. Cooperative localization of UAV based on information synchronization, in *2010 IEEE International Conference on Mechatronics and Automation, ICMA 2010*, pp. 225 - 230.
- Waharte, S., Trigoni, N., and Simon, J. S., Coordinated search with a swarm of UAVs, 2009. in *Proc. The 6th Annual IEEE Communications Society Conference on Sensor, Mesh and Ad Hoc Communications and Networks*, Rome, Italy.
- Wan, J., Zhong, L., and Zhang, F., 2014. Cooperative Localization of Multi-UAVs via Dynamic Nonparametric Belief Propagation under GPS Signal Loss Condition, *Int. J. Distrib. Sens. Networks*, pp. 1 - 10.
- Wanasinghe, T. R., Mann, G. K. I., and Gosine, R. G., 2014. Decentralized Cooperative Localization for Heterogeneous Multi-robot System Using Split Covariance Intersection Filter, in *Canadian Conference on Computer and Robot Vision*, pp. 167 - 174.
- Zheng, X., Jain, S., Koenig, S., and Kempe, D., 2005. Multi-robot forest coverage, *Intelligent Robots and Systems*, pp. 3852 - 3857.